Hindawi
Journal of Electrical and Computer Engineering
Volume 2022, Article ID 5897285, 12 pages
https://doi.org/10.1155/2022/5897285

Research Article

Security Enhancement of Power Systems through Interline Power Flow Controller (IPFC) under Contingency Condition: A Case Study and Analysis-EEP 400 kV System

Muluneh Lemma Woldesemayat[1] **and Ashenafi Tesfaye Tantu**[2]

[1]*Faculty of Electrical and Computer Engineering, Arba Minch University, Arba Minch, Ethiopia*
[2]*Department of Electrical and Computer Engineering, Wolaita Sodo University, Sodo, Ethiopia*

Correspondence should be addressed to Muluneh Lemma Woldesemayat; muluneh.lemma@amu.edu.et

Received 6 October 2022; Revised 9 November 2022; Accepted 10 November 2022; Published 30 November 2022

Academic Editor: Yang Li

Increasing contingency issues result in inevitable bus voltage violations and force the system to operate around its limit. This situation creates strains that are faced by the security of the Ethiopian Electric Power (EEP) 400 kV system. In this paper, the static security assessment (SSA) of the system under the base and N-1 contingency scenarios was examined by using Newton-Raphson (NR) method. The Bus and line loading-based composite severity indices (CSI) were utilized to determine the state of the system and to get an optimal location for interline power flow controller (IPFC) placement. In this research, the optimal sizing of IPFC was done by using Grey Wolf Optimization (GWO) algorithm. From N-1 contingency analysis, Gelan to Sebeta and Gelan to Holeta branches were found as optimal places for IPFC placement. The IPFC optimal parameters were the series voltage and angle injection found as V_{se1} = 0.1101pu, V_{se2}=0.1096pu, δ_{se1}=-0.1848rad, and δ_{se2}=2.7682rad with the optimal size of 50 MVA for each IPFC. The average bus voltage severity index (BVSI) without and with IPFC cases was found as 217.243% and 2.641% respectively. The average line severity index (LSI) without and with IPFC cases were found as 39.448% and 15.283% respectively. Moreover, the total line loss under severe N-1 contingency scenarios without and with IPFC integration was 437.783 MW and 63.136 MW respectively. From analysis, it was observed and concluded that the static security of the EEP 400 kV system under N-1 contingency conditions is effectively improved by the integration of IPFC.

1. Introduction

1.1. Background. A system that can tolerate the disruption of components without disrupting supply is called a secure system. The N-1 safety standard means that the operating system must withstand the failure of one component (may be a transmission line interruption or a generator unit) without violating the safe operating limits while supporting all the loads in the system [1].

The static security assessment is used for the prediction of line flows and bus voltages due to typical contingencies in a steady state. Static security specifies the security of the power system at a steady state after the occurrence of an outage of a line, a transformer, a generator, or a load from the system.

Contingency could be defined as failure of the system components, such as transmission line-related problems, which could be caused due to overloading or mal-operation of the transmission network, which leads the system component to fail [2]. The contingency analysis (CA) could be employed by the operators to assess the system security under component failures and to decide whether control actions are needed [3]. The computational complexity of contingency analysis may increase according to the number of components outage and it depends on the size of the system.

To maintain security limits, flexible AC transmission system (FACTS) device integration is found to be promising for modern power systems. The effectiveness of series compensation had been demonstrated in controlling line

power flow and improving stability [4]. An IPFC, which comprises multiple voltage source converters (VSCs), is one of the FACTS devices having the capacity of compensating for both real and reactive power flow through multiple transmission lines [2].

The proposed system in this paper consists of five 400 kV rated generation plants, 16 substations or buses (one slack bus, four voltage-controlled buses, and 11 load buses), 19 double-circuit transmission lines, four shunt reactors, and three shunt capacitors. Even though the systems are interconnected with each other by potential transmission lines; power system outage in Ethiopia is becoming a daily situation and resulting in higher system instability.

The EEP, the main concerned regulatory body for high voltage systems in Ethiopia, has the plan to reduce the system losses, which were also being considered for improvement of the system security by using under frequency load shedding scheme, installation of power quality meters for post-disturbance analysis, protection coordination studies to eliminate circuit trips due to errors and pole slip protection for generators [5].

1.2. Statement of the problem. According to contingency data collected from the EEP, the main events that trigger blackouts are (partial or total) reactive power supply shortages, outages of generation units, and line faults. Among those events, line faults and reactive power supply issues carry a higher weight and make the entire power system more unreliable than other isolated events. From 2017 to 2020, more than 256 outages occurred on EEP's 400 kV system due to line faults and operational issues. Most of the disruptions were related to lines (51.17%) and operation and maintenance issues (39.06%) and the remaining 9.77% were caused by miscellaneous problems. The loss reduction, reactive power compensation, and bus voltage profile improvement actions are still done by the shunt capacitors and reactors.

Research works on EEP national and regional power grids so far focused on reducing line losses by adding new transmission lines and/or improving their capacity. Although the system consists of double circuits, the power outages are not reduced sufficiently. Hence, in this study improvement is sought by conducting contingency management for a national 400 kV system using IPFC only considering transmission line outages.

1.3. Contribution of the study. The main objective of this study is power system static security improvement for EEP 400 kV system using IPFC integration during contingency situations.

1 The system static security investigation for base load and N-1 contingency case was conducted to determine the security state of the system.

2 The composite severity index (CSI) base analysis approach is proposed for contingency ranking since it is simple to formulate, requires less programming effort, have better computational efficacy than other optimization approaches.

3 The IPFC-based security enhancement was proposed due to its independent power flow control capability and its optimal parameters tuning done by using grey wolf optimization (GWO), which is selected due to its faster response, less memory requirement, and less programming effort.

4 From the study, it is shown that the static security of the EEP 400 kV system under N-1 contingency conditions with IPFC integration is improved.

2. Literature review

2.1. Review of related works. According to the North American Electric Reliability Council (NERC), "power system security is the ability of the electric system to withstand sudden disturbances such as electric short circuits or unanticipated loss of system elements." In other words, power system security implies the ability of a power system in normal operation mode to survive a likely disturbance without entering into an emergency state.

The power system security assessment is used to determine the healthiness of the system against possible contingencies during its operation. The security assessment of a power system includes steady state security assessment (SSA) and dynamic security assessment (DSA). The SSA focuses mainly on the buses, lines, and transformers' operating conditions when a typical contingency happens. Due to contingency, if the voltage profile for all the buses is within the predefined limit and no line is overloaded, then the network is said to be statically secure; otherwise, it is insecure [6].

The SSA, the main concern of this study, focuses on evaluating only the post-contingency steady state, ignoring time-dependent variations and transient behavior of the system. The DSA analyzes the dynamic behavior of the system in terms of transient or voltage stability when the system is subjected to perturbations. Moreover, the DSA focuses on system dynamics [3].

Nagesh et al. [7] proposed the maximization of power system static security in terms of branch loading and voltage level under normal and critical single-line contingency conditions by using optimally placed Thyristor-controlled series compensators (TCSCs) and static VAr compensators (SVCs) by using IEEE-30 bus as a test system.

Pallavi et al. [8] studied the implementation of multiple TCSCs for transmission line congestion reduction under the N-1 line contingency conditions. Optimal placement of TCSCs was conducted by using sensitivity analysis. Placing two TCSCs reduced line overloading, reactive power loss, and voltage profile improvement in the IEEE-14 bus system.

Kavuturu et al. [9] examined the impact of the optimally placed unified power flow controller (UPFC) during N-1 line contingency on transmission system security. To test the UPFC performance under N-1 contingency conditions, the power flow was formulated using a line collapse proximity indicator (LCPI) and then an N-1 contingency analysis was performed by considering the UPFC device at different RES generation levels.

Tong et al. [10] proposed the TCSC and SVC to maximize static security in terms of branch loading and voltage limits under normal and the most critical N-1 contingency conditions. The tangent vector technique (TVT) and cuckoo search algorithm (CSA) were employed to determine the proper candidate location and optimal size settings. The IEEE 6-bus and modified IEEE 14-bus were used as test systems.

Frezer [11] conducted an N-1 contingency study on the EEP southern region using UPFC to reduce line losses, line overloading, and bus voltage improvement. The optimal placement and sizing of UPFC were calculated by the loss sensitivity index and PSO algorithm.

Natnael [12] conducted a study on EEP 400 kV and 230 kV systems to assess transmission line loss under base and N-1 line contingency cases using the PowerWorld simulator. To reduce the system loss under the N-1 line contingency condition, the addition of transmission lines and shunt capacitor-based compensation solutions were proposed.

Genanew [13] performed the contingency analysis for EEP 230kV and 400kV systems by considering power performance indices (PPI) for transmission line outages utilizing the PSS/E software. Upgrading the existing single-circuit transmission lines to double circuits and adding capacitor-based compensation were proposed as mitigation approaches to make the power system to be secure.

Gezahegn [14] conducted the security enhancement study of the EEP HV system using UPFC. The system was simulated under transmission line outage and their criticalities were ranked by using the line stability index (LSI) and active power performance index (APPI). The feasible locations for the UPFC deployment are identified using CSI by using MATLAB.

Li et al. [15] proposed the LASSO algorithm for online static security assessment based on a security index to select and screen the contingencies. The proposed algorithm was employed to predict the security index considering the bus voltages and power flows in post-contingency states by utilizing the NR method considering the IEEE 14-bus, 118-bus, and 300-bus systems as test systems.

Desalegn et al. [16] performed contingency analysis by employing the active power performance index (APPI) and reactive power performance index (RPPI) during a single line outage for the EEP North-West region with DIgSILENT simulation software. Based on the load flow results, series compensators were proposed as a compensation approach.

Krishna et al. [17] proposed the composite severity index (CSI) formed by using the Line utilization factor (LUF) and Line stability index (LSI) to evaluate line overloads and bus voltage violations. LUF is used for the measurement of line overloads in terms of MVA line flows and LSI is used for the assessment of bus voltage stability in the IEEE-30 bus system.

Li et al. [18] proposed security-constrained multi-objective optimal power flow (SC-MOPF) to coordinate the economy and voltage quality of a meshed AC/VSC-MTDC system with Lasso-Based Contingency filtering. A novel bi-criterion evolution indicator-based evolutionary algorithm (BCE-IBEA) is developed to seek multiple well-spread Pareto-optimal solutions through the introduction of parallel computation. The LASSO-based N-1 contingency ranking approach with a CSI was developed to identify the most severe contingency. The modified IEEE 14- and 300-bus systems were utilized to demonstrate the proposed approach.

Neural networks (NNs) as one of the computational methods for the selection of contingencies in static security analysis is proposed in [19–21] to estimate the post-contingency state of the power system. The results presented showed satisfactory results for small to medium power systems, concerning single-branch outages.

2.2. Identified Research gap. It has been shown that intelligent soft computing techniques can meet the large computational burden that many analytical models fail to meet. However, it is believed that intelligent soft computing techniques become less effective as power system size increases. Several papers have reported contingency rating approaches, but indices based on line loading and bus voltage deviations revealed enough capability and achieved high performance in identifying and selecting the most severe contingency. In addition, the proposed approach is simple and requires less programming effort than other complex programming approaches.

Optimization algorithms are highly recommended as the location and size of FACTS devices pose a non-routine optimization problem due to various operating constraints. Several optimization algorithms have been proposed to optimize the FACTS devices to overcome the contingency problem. However, the GWO has a faster response time, less memory requirement, and requires a simpler programming approach than the GA, PSO, GSA, and WOA algorithms [22–24], thus it is gaining higher attention recently in power systems.

The approach presented in this study is a CSI-based emergency analysis that includes two types of indices: (1) Bus Voltage Severity Index (BVSI) and (2) Line Severity Index (LSI). Hence, these indices can provide the clear current operating status of the power system under various conditions. The BVSI consists of voltage performance index (VPI) and voltage deviation index (VDI) indices while the LSI is made using LUF and NLSI indices. The proposed approach is limited to considering only the bus voltage magnitude deviation margin and line loading state during an outage of the transmission lines only. The proposed approach may have a limitation on the determination of the time-dependent variables, like the frequency which are the usual parameters varying with the system loading condition.

The SVC, STATCOM, TCSC, SSSC, and UPFC devices have the capability of compensating for a single transmission line. However, they are unable to control both active and reactive power flow independently through the branch except UPFC. Unlike the UPFC, IPFC has gained higher performance for power flow management in the case of the multi-line system.

Table 1: Existing ICS 400 kV rated hydropower plants.

No	Station	Units	U1 (kV)	U2 (kV)	Prated (MW)	Qmin (Mvar)	Qmax (Mvar)
1	Beles	4	15	400	460	-230	230
2	GGnew	3	13.8	400	100	-63	63
3	GG II	4	15	400	420	-200	200
4	GG III	10	15	400	1870	-1000	1000
5	GD III	3	13.8	400	254	-160	160

Table 2: Transmission line parameters of 400 kV system.

No	From	To	R (pu)	X (pu)	B (pu)	S (MVA)
1	GG3	W/Sodo	0.0010	0.0081	0.0004	1973
2	W/Sodo	GG2	0.0025	0.0207	0.0010	1973
3	W/Sodo	Gelan	0.0055	0.0432	0.0024	1973
4	W/Sodo	Yirgalem	0.0024	0.0197	0.0009	1973
5	GG2	Sebeta	0.0028	0.0378	0.0013	1341
6	GG2	GGnew	0.0004	0.0057	0.0002	1341
7	Gelan	Sebeta	0.0007	0.0057	0.0003	1973
8	Gelan	Holeta	0.0010	0.0079	0.0004	1973
9	Gelan	D/Zeit	0.0006	0.0049	0.0003	1973
10	Sebeta	Holeta	0.0003	0.0034	0.0001	1973
11	Holeta	Sululta	0.0006	0.0050	0.0003	1973
12	Sululta	D/Markos	0.0033	0.0444	0.0015	1341
13	Sululta	D/Zeit	0.0018	0.0137	0.0006	1973
14	Sululta	G/Gurcha	0.0020	0.0271	0.0009	1341
15	D/Markos	B/Dar	0.0030	0.0399	0.0014	1341
16	D/Markos	G/Gurcha	0.0014	0.0180	0.0006	1341
17	B/Dar	Beles	0.0010	0.0122	0.0005	1341
18	Beles	GERD	0.0045	0.0460	0.0018	1973
19	Yirgalem	GD3	0.0057	0.0444	0.0024	1973

Table 3: Base load data as of 2021.

No	Station	Region	P (MW)	Q (Mvar)
1	GG3	SW	458.69	123.51
2	W/Sodo	South	335.92	150.57
3	GG2	SW	53.21	22.3
4	Gelan	AA	205	95.56
5	Sebeta	AA	239.6	110.3
6	Holeta	Center	89.38	40.63
7	Sululta	AA	153.68	62.87
8	D/Markos	NW	98.21	46.35
9	B/Dar	NW	143.53	50.76
10	Beles	North	20.87	6.33
11	GERD	NW	70.22	26.24
12	D/Zeit	Center	124.73	63.32
13	Yirgalem	South	56.36	39.25
14	GD3	South	73.75	30.03
15	G/Gurcha	North	31.62	14.17
16	GGnew	SW	47.22	25.63
Total			**2201.99**	**907.82**

3. Methodology

3.1. EEP grid modeling. The Ethiopian electric power system has two major systems, ICS (Interconnected System) and SCS (self-contained system). Currently, it has a total installed capacity of 4071 MW from hydro (Source: EEP generation operation department). The data required for this study were collected from the Ethiopian NLDC. For some critical disturbances, the sequence of events observed on the SCADA was reviewed from the NLDC archive. For this study, only 400 kV-rated power plants were considered to have a total capacity of 3188 MW as shown in Table 1.

The collected data of 400 kV system transmission lines were filtered and converted to per-unit values at 100 MVA and 400 kV base power and voltage levels as shown in Table 2.

The active and reactive power load data for the entire 400 kV system were collected and rescaled as shown in Table 3, having a total base load demand of 2201.99 MW and 907.82 MVAR.

Shunt reactors and capacitors are installed at different locations in the existing 400 kV system as shown in Table 4. Here, some devices, which are not in use and currently broken, are not included.

Table 4: Parameters of reactive power compensators.

No	Name	Shunt Device	Rating (MVAR)
1	Sululta	Reactor	1x45
2	B/Dar	Reactor	1x45
3	D/Markos	Reactor	1x45
4	GGnew	Reactor	1x45
5	Sebeta	Capacitor	1x90
6	Gelan	Capacitor	1x90
7	W/Sodo	Capacitor	1x90

3.2. NR load flow analysis. The procedure for power flow solution by using the NR method is shown below:

(i) Step 1: Specify the active and reactive power for load buses and set voltage magnitudes and phase angles to 1 and 0. For voltage-controlled buses, specify the voltage magnitude and power rating and set phase angles to 0.

(ii) Step 2: Initialize the system parameters and start the iterations.

(iii) Step 3: Calculate the power injections and power mismatch for each load bus.

(iv) Step 4: For voltage-controlled buses, calculate the active power flow and its mismatch vector.

(v) Step 5: Calculate the Jacobian matrix.

(vi) Step 6: Calculate the new voltage magnitudes and phase angles for all buses. Calculate the line flows for all branches.

(vii) Step 7: Continue the process until the accuracy level is reached.

(viii) Step 8: If the system converged for the given accuracy and iteration level, end the process and display the results.

The same procedure could be used for the contingency analysis by removing the contingent branch and recalculating the admittance matrix for the remaining system. The other steps are the same as the steps shown above for the NR-load flow method.

3.3. Composite Severity Index (CSI) Formulation. Formulation of the composite severity index (CSI) comprises consideration of the line parameter-based indices and bus voltage magnitude indices. The line severity indices (LSI) considered for this thesis are line utilization factor (LUF) and novel line stability index (NLSI). The bus voltage severity indices (BVSI) considered for this thesis are the voltage deviation index (VDI) and voltage performance index (VPI).

3.3.1. Line Utilization Factor (LUF). Line utilization factor (LUF) proposed in [25] is the measure of utilization of a particular line. The LUF uses apparent power for the calculation of line loading as given as follows:

$$\mathrm{LUF}_{ij} = \frac{\mathrm{MVA}_{ij}}{\mathrm{MVA}_{ij\max}}, \tag{1}$$

where LUF_{ij} is the line utilization factor of the line connected to bus-i and bus-j; $\mathrm{MVA}_{ij\max}$ is the maximum MVA rating of the line between bus-i and bus-j; MVA_{ij} is the actual MVA rating of the line between bus-i and bus-j; L is the no. of lines in the system. The LUF should be less than unity for secure operation.

3.3.2. Novel Line Stability Index (NLSI). The NLSI presented in [26] is used for determining the point of voltage collapse, identification of weak bus, and the most critical line in a system. The NLSI considers both active and reactive power flow to investigate the voltage stability because it could be better to consider both active and reactive power flow than to consider only reactive power flow.

$$\mathrm{NLSI}_{ij} = \frac{R_{ij}P_j + X_{ij}Q_j}{0.25V_i^2}, \tag{2}$$

where V_i is the voltage at the sending end bus; P_j and Q_j are the active and reactive power at the receiving end bus; R_{ij} and X_{ij} are the line resistance and reactance between sending and receiving end buses, respectively. To maintain a secure system, NLSI should be less than unity.

The line severity index (LSI) could be formulated by using LUF and NLSI as follows:

$$\mathrm{LSI}_{ij} = w_1\mathrm{LUF}_{ij} + w_2\mathrm{NLSI}_{ij}, \tag{3}$$

where w_1 and w_2 are weighting factors with values of 0.7 and 0.3 for each. For secure operation, the LSI should be less than unity.

3.3.3. Voltage Deviation Index (VDI). This index gives the measure of the bus voltage index by comparing the actual bus voltage with the nominal voltage value. The VDI for a bus-i is given as follows:

$$\mathrm{VDI}_i = \left|\frac{V_{\mathrm{ref}} - V_{\mathrm{bus}}}{V_{\mathrm{ref}}}\right| \times 100\%, \tag{4}$$

where V_{bus} is the actual bus voltage and V_{ref} is the nominal bus voltage. The VDI should not be greater than 5% for secure operation.

3.3.4. Voltage Performance Index (VPI). The VPI describes the stability of a bus voltage magnitude. The VPI for a bus-i is given as follows:

$$\mathrm{VPI}_i = \left|\frac{V_{\mathrm{bus}} - V_{\mathrm{ref}}}{V_{\max} - V_{\min}}\right|^2, \tag{5}$$

where $V_{\min}$ and $V_{\max}$ are min and max limits with values 0.95 and 1.05 pu, respectively. The VPI should be less than 25% to maintain secure bus voltage magnitude.

$$\mathrm{BVSI}_i = w_1\mathrm{VDI}_i + w_2\mathrm{VPI}_i, \tag{6}$$

where w_1 and w_2 are weighting factors with values of 0.4 and 0.6. When the index value approaches one, it implies that the bus is going to be unstable.

Both LSI and BVSI indices have been considered to formulate a CSI for each line and bus. Each CSI value should be less than unity for the system to be secure. The steps employed for CA using CSI are shown as follows:

(i) Step 1: initialize the system parameters.

(ii) Step 2: perform the load flow for the pre-contingency condition.

(iii) Step 3: create a typical contingency (branch outage in our case).

(iv) Step 4: perform the load flow for postcontingency condition.

(v) Step 5: compute a CSI for each defined branch contingency.

(vi) Step 6: if all the outages are considered, rank the contingencies according to the CSI values, otherwise go to step 3 and repeat the same steps.

(vii) Step 7: display the results.

3.4. Power flow modeling with IPFC. The equivalent circuit of IPFC within the system is shown in figure 1. From the figure, $\mathbf{V}_{\mathrm{i}} = \mathrm{V}_{\mathrm{i}}\angle\theta_{\mathrm{i}}$, $\mathbf{V}_{\mathrm{j}} = \mathrm{V}_{\mathrm{j}}\angle\theta_{\mathrm{j}}$, and $\mathbf{V}_{\mathrm{k}} = \mathrm{V}_{\mathrm{k}}\angle\theta_{\mathrm{k}}$ are the voltages of the buses i, j, and k respectively with V_{L} and θ_{L} being the magnitude and phase angle of $\mathbf{V}_{\mathrm{L}}$ (L = i, j, k). The unknown

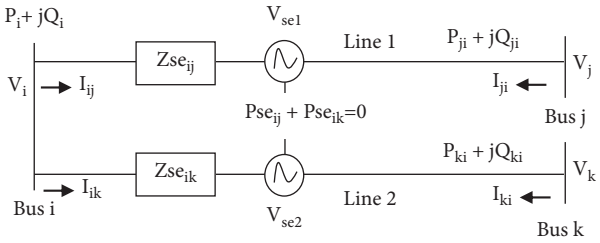

Figure 1: Equivalent circuit of IPFC.

IPFC variables V_{sep}, θ_p (p = 1,2) can be determined from the power flow equations:

$$\left.\begin{aligned} P_{ni} &= V_n^2 g_{in} - V_n V_i \left(g_{in}\cos\left(\theta_n - \theta_i\right) + b_{in}\sin\left(\theta_n - \theta_i\right)\right) \\ &\quad + V_{sep} V_n \left(g_{in}\cos\left(\theta_n - \theta_p\right) + b_{in}\sin\left(\theta_n - \theta_p\right)\right) \\ Q_{ni} &= -V_n^2 b_{in} + V_n V_i \left(g_{in}\sin\left(\theta_n - \theta_i\right) - b_{in}\cos\left(\theta_n - \theta_i\right)\right) \\ &\quad + V_{sep} V_n \left(g_{in}\sin\left(\theta_n - \theta_p\right) + b_{in}\cos\left(\theta_n - \theta_p\right)\right) \end{aligned}\right\}, \tag{7}$$

where g_{in} and b_{in} are the conductance and susceptance between bus i and n.

The NR-load flow implementation of the power system incorporated with IPFC is developed in [27] and is summarized as shown in the following steps.

(i) Step 1: Specify the proposed power system data.

(ii) Step 2: Initialize the system control parameters.

(iii) Step 3: Start the iteration to compute the power flows at all the buses.

(iv) Step 4: Compute the power mismatches at each bus.

(v) Step 5: If the power mismatch is less than the tolerance limit, go to step 10 else go to step six.

(vi) Step 6: Form the Jacobian matrix parameters by including the IPFC parameters.

(vii) Step 7: Update IPFC injected bus voltage magnitudes and angles simultaneously.

(viii) Step 8: Check whether all constraints are satisfied. If constraints are violated, set parameters at the limited values.

(ix) Step 9: Increase the iteration count and go to step four.

(x) Step 10: If the load flow is converged, print the power flow results.

3.5. Optimal sizing of IPFC with GWO

3.5.1. Objective function formulation

(1) Minimization of bus voltage severity margin:

To have a good voltage performance, the voltage deviation (VD) at each bus must be made as small as possible [28] as given by:

$$F_1 = \min \sum_{i=1}^{N\text{bus}} \left| \frac{V_{\text{ref}} - V_{\text{bus}}}{V_{\text{ref}}} \right|, \tag{8}$$

where V_{ref} and V_{bus} are the references and actual bus voltage magnitudes.

(2) Minimization of line severity margin

The security level of the system can be identified by the severity of the contingency. The security level of a system according to the critical state can be expressed in [25] as:

$$F_2 = \min \sum_{j=1}^{N_{\text{branch}}} \frac{S_j}{S_{j,\text{rated}}}. \tag{9}$$

where S_j and $S_{j,rated}$ are actual and rated MVA for branch j.

(3) Minimization of the active power loss

The third objective is to minimize the power loss that could be raised due to contingency given by:

$$F_3 = \min \sum_{j=1}^{N_{\text{branch}}} P_{\text{loss}}. \tag{10}$$

3.5.2. Constraints formulation. The proposed optimization tested with the following equality load flow constraints, bus voltage, and the IPFC limit inequality constraints.

(1) Equality constraints: represents typically the power balance equations

$$\left.\begin{aligned} P_{k\text{gen}} - P_{k\text{load}} - P_{k\text{loss}} &= 0 \\ Q_{k\text{gen}} - Q_{k\text{load}} - Q_{k\text{loss}} &= 0 \end{aligned}\right\}, \tag{11}$$

where P_{kgen} and Q_{kgen} are the active and reactive powers generated at node k, P_{kload} and Q_{kload} are the active and reactive powers consumed by the load at node k; P_{kloss} and Q_{kloss} are the calculated active and reactive powers losses at node k.

(2) Inequality constraints: represents the variable limit of the system.

$$\left.\begin{aligned} V_{i\min} &\le V_i \le V_{i\max} \\ V_{se-\min} &\le V_{se} \le V_{se-\max} \\ \theta_{se-\min} &\le \theta_i \le \theta_{se-\max} \end{aligned}\right\}, \tag{12}$$

Where $V_{i,min}$ and $V_{i,max}$ are the bus voltage lower and upper limits with the values of 0.95 and 1.05 respectively and V_{se} is the series injected voltage magnitude, $\theta_{se\text{-}min} = -\pi$ and $\theta_{se\text{-}max} = \pi$.

4. Results and discussions

The EEP 400 kV power system is simulated for two scenarios: base load and N-1 contingency. The outage considered in this study was only the line outage. For each case, the bus voltage and line loading limits are checked with tolerance limit values. Finally, the weakest buses and branches are selected as candidates for IPFC integration.

A full N-1 contingency simulation is performed to identify the most severe branch that makes the system unsafe. Since the test system consists of 19 branches, it is not recommended to list all the contingency results due to space and time limitations, so the most severe branch contingency analysis was carried out with the help of MATLAB software.

The 8GB RAM hp laptop computer with Intel(R) Core(TM) i7-7500U CPU @ 2.70GHz processor has been used to run the power flow program. The NR power flow solution was utilized at 100MVA and 400kV base power and base voltage with the considered accuracy of $1x10^{-4}$ and 100 iterations.

Since the system does not operate in peak load conditions the entire time; base load data is preferred for contingency simulation. Uploading the base load data in the NR-base power flow program, the contingency was created one by one for all 19 branches.

The branch identified as a severe branch during the N-1 contingency risk analysis is the Sebeta to Holeta branch which caused the highest bus voltage magnitude violation, the highest rate of line overloading state, and the highest power loss among other branches in the system. Therefore, the analysis proposed to demonstrate the N-1 contingency is performed on the termination of this branch.

4.1. Simulation without IPFC. The power flow program terminated and resulted in the maximum power mismatch of 8.866 x10-6 by taking eight iterations.

4.1.1. Bus voltage severity index. The resulting bus voltages for the base load and N-1 case without IPFC integration are shown in Table 5. From the result, we can see that no bus voltage is violated under steady-state base load conditions. The voltage levels of the Gelan and Sebeta buses were significantly reduced during the N-1 contingency simulation.

The VDI, VPI, and BVSI for all buses in the system should not exceed 5%, 25%, and 17% for safe operation. The lower the BVSI value, the higher the safety of the bus voltage. In other words, if the BVSI value is approaching zero, the severity of the bus voltage violation is small. However, from Table 6, VDI, VPI, and BVSI for Gelan, Sebeta, D/Markos, and D/Zeit buses were found to be far beyond the required limit for severe N-1 case simulation. Therefore, safe operation is not guaranteed when the Sebeta to Holeta branch is disconnected from the system.

Table 5: Bus voltage magnitude and phase angle without IPFC.

Buses		Base case scenario		N-1 case scenario	
No	Name	V (pu)	Ang (deg)	Vbus (pu)	Ang (deg)
1	GG3	1.0000	0	1.0000	0
2	W/Sodo	0.9985	−2.25780	0.9485	−1.0000
3	GG2	1.0000	−1.49840	1.0000	−2.8906
4	Gelan	0.9630	−10.5423	0.5910	−3.0022
5	Sebeta	0.9624	−10.4323	0.4080	−2.9273
6	Holeta	0.9626	−10.6696	0.9530	−3.0634
7	Sululta	0.9667	−10.9049	1.0310	−3.0945
8	D/Markos	0.9805	−9.54770	0.8770	−3.1952
9	B/Dar	0.9921	−4.32070	0.9690	−3.3083
10	Beles	1.0000	−1.74680	1.0000	−3.3268
11	GERD	1.0018	−3.25300	0.9690	−3.3297
12	D/Zeit	0.9639	−10.9188	0.8370	−3.0508
13	Yirgalem	1.0141	−0.56040	0.9760	−2.0524
14	GD3	1.0164	−1.00790	1.0000	−2.1152
15	G/Gurcha	1.0040	−3.63030	0.9640	−3.1710
16	GGnew	1.0000	−1.17030	1.0000	−2.8943

Table 6: BVSI during an outage of Sebeta to the Holeta branch without IPFC.

No	Name	Vref	Vact	VDI (%)	VPI (%)	BVSI (%)
1	GG3	1	1	0	0	0
2	W/Sodo	1	0.9485	5.15	26.5225	17.9735
3	GG2	1	1	0	0	0
4	Gelan	1	0.591	40.9	1672.81	1020.046
5	Sebeta	1	0.408	59.2	3504.64	2126.464
6	Holeta	1	0.953	4.7	22.09	15.134
7	Sululta	1	1.031	3.1	9.61	7.006
8	D/Markos	1	0.877	12.3	151.29	95.694
9	B/Dar	1	0.969	3.1	9.61	7.006
10	Beles	1	1	0	0	0
11	GERD	1	0.969	3.1	9.61	7.006
12	D/Zeit	1	0.837	16.3	265.69	165.934
13	Yirgalem	1	0.976	2.4	5.76	4.416
14	GD3	1	1	0	0	0
15	G/Gurcha	1	0.964	3.6	12.96	9.216
16	GGnew	1	1	0	0	0

4.1.2. Line severity index and losses. The Total active and reactive power losses were found to be 32.976 MW and 105.215 MVAR respectively for base load conditions without IPFC. The active and reactive power losses encountered during the disconnection of the Sebeta to Holeta branch were found to be 437.783MW and 254.779 MVAR. The LSI is calculated as shown in Table 7.

From Table 7, the LSI for W/Sodo to Gelan and Gelan to Holeta branches at the cut-off case from Sebeta to Holeta branch resulted in higher LSI values than the other branches. The line from GG3 to W/Sodo, W/Sodo to Gelan, Gelan to Sebeta, and Gelan to Holeta branches were loaded at 108.099%, 102.655%, 104.468%, and 106.373%, respectively. This proved almost the same result as the real-time system operating state during an outage of Sebeta to the Holeta branch.

Table 7: LSI during an outage of Sebeta to the Holeta branch without IPFC.

From	To	Actual MVA	Rated MVA	LUF (%)	NLSI (%)	LSI (%)
GG3	W/Sodo	2132.794	1973	108.099	34.1900	85.926
W/Sodo	GG2	1221.193	1973	61.8950	57.0110	60.430
W/Sodo	Gelan	2025.377	1973	102.655	153.159	117.806
W/Sodo	Yirgalem	171.2350	1973	8.67900	6.34400	7.979
GG2	Sebeta	140.7990	1341	10.5000	12.1800	11.004
GG2	GGnew	90.96300	1341	6.78300	0.8220	4.995
Gelan	Sebeta	2061.160	1973	104.468	56.546	90.092
Gelan	Holeta	2098.737	1973	106.373	87.336	100.662
Gelan	D/Zeit	1289.108	1973	65.3370	42.359	58.444
Sebeta	Holeta	0	1973	0	0	0
Holeta	Sululta	831.8770	1973	42.1630	7.797	31.853
Sululta	D/Markos	355.3140	1341	26.4960	25.254	26.124
Sululta	D/Zeit	811.2700	1973	41.1190	25.938	36.564
Sululta	G/Gurcha	208.0350	1341	15.5130	7.929	13.238
D/Markos	B/Dar	390.3600	1341	29.1100	40.433	32.507
D/Markos	G/Gurcha	559.0270	1341	41.6870	7.840	31.533
B/Dar	Beles	357.8380	1341	26.6840	8.683	21.284
Beles	GERD	97.15600	1973	4.92400	8.754	6.073
Yirgalem	GD3	208.8480	1973	10.5850	18.631	12.999

Finally, we can say that the proposed power system cannot maintain safety under N-1 contingency issues. Therefore, the technique is required to maintain the static security requirement of the system. The main issue that arises is the bus voltage, which is not kept within the tolerance limit in all N-1 conditions. Since the voltage and reactive power are related to each other, if the bus voltage is not maintained at the tolerance limit, the system loss may be greater and result in an inefficient system.

4.2. Simulation with IPFC. Before the integration of the IPFC, according to the N-1 contingency analysis, the buses connected to the Gelan bus caused higher voltage instability. Therefore, the Gelan bus can be considered the primary bus of IPFC integration. From the CSI analysis, the Gelan to Sebeta and Gelan to Holeta branches were considered suitable locations.

The number of wolves considered was 12 with four variables, namely series voltage injection (V_{se1} and V_{se2}) and voltage injection phase angles (θ_{se1} and θ_{se2}). The code was developed in MATLAB script and the optimal parameters were found to be V_{se1} = 0.1100pu and V_{se2} = 0.1096pu, θ_{se1} =-0.1848rad and θ_{se2} = 2.7682rad with the optimal MVA rating of $MVA_{45}^{IPFC} = 0.3647\,pu$ and $MVA_{46}^{IPFC} = 0.4647\,pu$. Then the power rating is the maximum of the two VSCs, which could be 0.4647 pu$*$100 MVA = 46.47 MVA for each IPFCs. From this, the 50 MVA rated IPFC is connected between Gelan to Sebeta and Gelan to Holeta branches as shown in Figure 2.

4.2.1. Bus voltage severity index. From Table 8, we can see that the voltage levels of Gelan, Sebeta, Sululta, D/Markos, and D/Zeit buses were safe during the outage of the Sebeta to Holeta branch. These buses experienced very much lower voltages without the IPFC case.

As shown in Table 9, we can see that the resulting VDI, VPI, and BVSI for all buses in the system is less than the safe operating tolerance of 5%, 25%, and 17% respectively. Therefore, the inclusion of IPFC within the system has improved the bus voltage and more importantly reduced the severity of the bus voltage profile violation. The outage from Sebeta to the Holeta branch has resulted in a high bus voltage magnitude violation problem without an IPFC case on all central region buses. However, the integration of IPFC in the system significantly improved the BVSI for all system buses, resulting in reliable normalized values.

4.2.2. Line severity index and losses. For base load condition with IPFC, the total active and reactive power losses were found to be 19.919MW and 66.389 MVAR respectively, while the power loss during the disconnection from Sebeta to Holeta branch was found to be 63.136 MW and 105.424 MVAR. Based on the simulation results with IPFC, the LSI is calculated as shown in Table 10.

We can see from Table 10 that the LSI with IPFC has resulted in less than 100% reliable LSI value for all branches during the outage of Sebeta to the Holeta branch. From the results, we can conclude that IPFC integration has improved the static security issues under N-1 contingency.

4.3. Comparative analysis

4.3.1. Bus voltage severity index (BVSI). The VDI values for Gelan, Sebeta, D/Markos, and D/Zeit buses are 40.9%, 59.2%, 12.3%, and 16.3% respectively, which is far from the maximum tolerance limit of 5%. Similarly, the VPI for those buses was found to be 1672.81%, 3504.64%, 151.29%, and 265.69% respectively, which is much greater than the secure limit of 25%, which confirms that the system is at risk.

The BVSI for Gelan, Sebeta, D/Markos, and D/Zeit buses is found to be 1020.046%, 2126.464%, 95.694%, and 165.934% respectively as shown in Figure 3, which is higher than the safe tolerance limit set of 17% during severe N-1 emergency condition without IPFC.

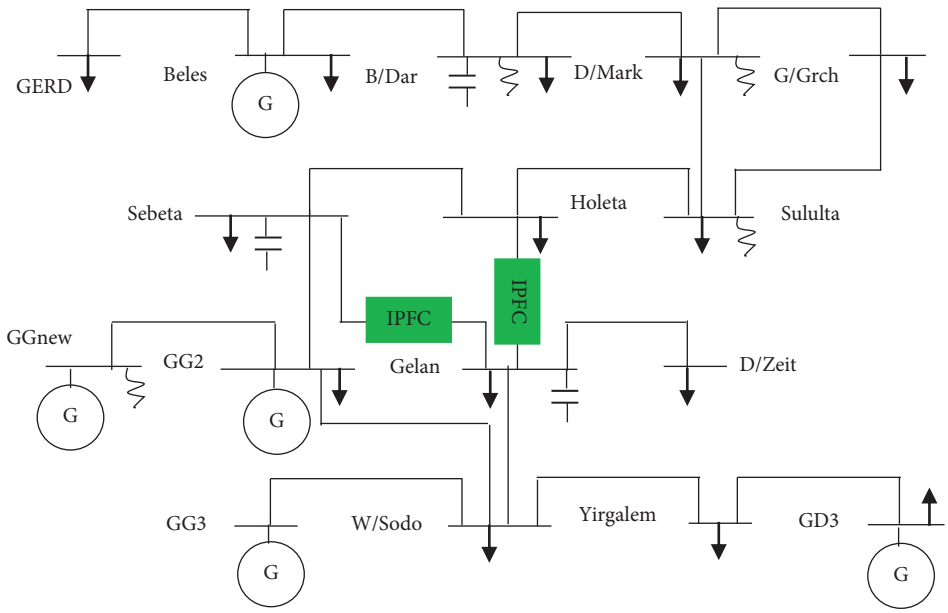

Figure 2: Proposed power system with IPFC.

Table 8: Bus voltage magnitude and phase angle with IPFC.

Buses		Base case scenario		N-1 case scenario	
No	Name	Vbus (pu)	Ang (deg)	Vbus (pu)	Ang (deg)
1	GG3	1	0	1	0
2	W/Sodo	1.0099	−2.32586	1.047	−0.0868
3	GG2	0.9997	−1.50792	1	−0.1846
4	Gelan	0.9836	−10.3944	1	−0.3288
5	Sebeta	0.9839	−10.2937	1	−0.3104
6	Holeta	0.9863	−10.5381	0.985	−0.3333
7	Sululta	0.9923	−10.775	0.9804	−0.3359
8	D/Markos	1.0055	−9.50964	1.0047	−0.3541
9	B/Dar	0.9984	−4.40367	1.0161	−0.3839
10	Beles	0.9995	−1.81031	1	−0.3921
11	GERD	1.0001	−3.31649	0.9695	−0.3935
12	D/Zeit	0.9852	−10.7558	0.9687	−0.331
13	Yirgalem	1.0396	−1.19638	1.013	−0.091
14	GD3	1.0486	2.98491	1	−0.099
15	G/Gurcha	1.0114	−10.2523	0.977	−0.3471
16	GGnew	0.9998	−1.17979	1	−0.1883

Table 9: BVSI during an outage of Sebeta to the Holeta branch with IPFC.

No	Name	Vref	Vact	VDI (%)	VPI (%)	BVSI (%)
1	GG3	1	1	0	0	0
2	W/Sodo	1	1.047	4.7	22.09	15.134
3	GG2	1	1	0	0	0
4	Gelan	1	1	0	0	0
5	Sebeta	1	1	0	0	0
6	Holeta	1	0.985	1.5	2.25	1.95
7	Sululta	1	0.9804	1.96	3.8416	3.089
8	D/Markos	1	1.0047	0.47	0.2209	0.321
9	B/Dar	1	1.0161	1.61	2.5921	2.199
10	Beles	1	1	0	0	0
11	GERD	1	0.9695	3.05	9.3025	6.801
12	D/Zeit	1	0.9687	3.13	9.7969	7.130
13	Yirgalem	1	1.013	1.3	1.69	1.534
14	GD3	1	1	0	0	0
15	G/Gurcha	1	0.977	2.3	5.29	4.094
16	GGnew	1	1	0	0	0

The VDI, VPI, and BVSI for Gelan, Sebeta, D/Markos, and D/Zeit buses decreased below the 5%, 25%, and 17% safe tolerance limit under severe N-1 contingency conditions with IPFC integration. Moreover, the overall system average VDI, VPI, and BVSI values without IPFC incorporation during severe N-1 contingency scenario is found to be 9.616%, 355.662%, and 217.243% respectively. However, these values with the IPFC case are found to be 1.251%, 3.567%, and 2.641% respectively.

4.3.2. Line severity index (LSI). The LSI values for W/Sodo to Gelan, Gelan to Holeta, Gelan to Sebeta, and GG3 to W/Sodo branches during the severe N-1 contingency case without IPFC integration are 117.806%, 100.662%, 90.092%, and 85.926%, respectively as shown in Figure 4.

However, integrating IPFC into the system has resulted in lower line overloading margins for all system branches. The LSI from W/Sodo to Gelan, Gelan to Holeta, Gelan to Sebeta, and GG3 to W/Sodo branches in a severe N-1 contingency case with IPFC condition is well below the 100% safe tolerance limit.

Moreover, the overall system average VDI, VPI, BVSI, LUF, NLSI, and LSI values for severe N-1 contingency situations without IPFC were found to be 9.616%, 355.662%, 217.243%, 42.793%, 31.642%, and 39.448%, respectively. However, these values with the IPFC integration scenario were found to be 1.251%, 3.567%, 2.641%, 17.183%, 10.851%, and 15.283% respectively as shown in Table 11 and Figure 5.

Table 10: LSI during an outage of Sebeta to the Holeta branch with IPFC.

From	To	Actual MVA	Rated MVA	LUF (%)	NLSI (%)	LSI (%)
GG3	W/Sodo	791.158	1973	40.099	15.007	32.572
W/Sodo	GG2	166.666	1973	8.447	7.958	8.301
W/Sodo	Gelan	540.544	1973	27.397	53.273	35.160
W/Sodo	Yirgalem	134.246	1973	6.804	5.437	6.394
GG2	Sebeta	111.157	1341	8.289	7.751	8.128
GG2	GGnew	51.940	1341	3.873	0.533	2.871
Gelan	Sebeta	745.080	1973	37.764	11.432	29.864
Gelan	Holeta	186.858	1973	9.471	2.046	7.243
Gelan	D/Zeit	313.985	1973	15.914	2.243	11.813
Sebeta	Holeta	0.000	1973	0.000	0.000	0.000
Holeta	Sululta	547.526	1973	27.751	3.198	20.385
Sululta	D/Markos	156.883	1341	11.699	20.285	14.275
Sululta	D/Zeit	306.821	1973	15.551	7.875	13.248
Sululta	G/Gurcha	199.738	1341	14.895	8.369	12.937
D/Markos	B/Dar	342.632	1341	25.550	22.809	24.728
D/Markos	G/Gurcha	480.879	1341	35.860	9.807	28.044
B/Dar	Beles	350.024	1341	26.102	8.808	20.914
Beles	GERD	86.173	1973	4.368	7.007	5.159
Yirgalem	GD3	130.894	1973	6.634	12.339	8.346

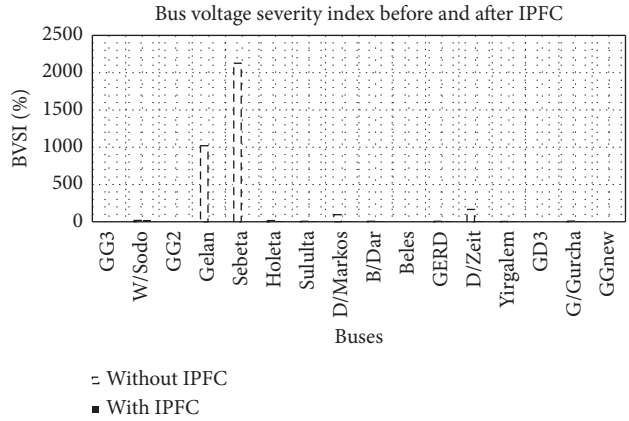

Figure 3: Bus voltage severity index before and after IPFC.

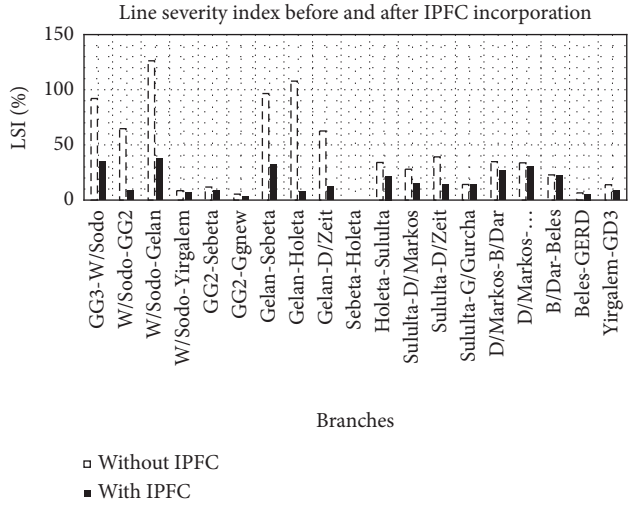

Figure 4: Line severity index before and after IPFC incorporation.

Table 11: Overall severity indices comparison for an N-1 contingency case.

Indices	Without IPFC	With IPFC
VDI (%)	9.616	1.251
VPI (%)	355.662	3.567
BVSI (%)	217.243	2.641
LUF (%)	42.793	17.183
NLSI (%)	31.642	10.851
LSI (%)	39.448	15.283

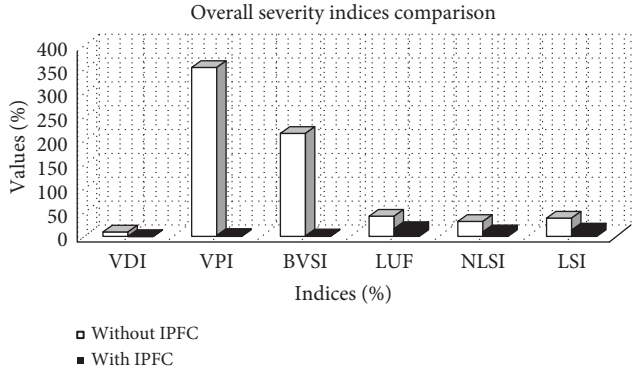

Figure 5: Overall severity indices comparison for a severe N-1 contingency case.

5. Conclusion

In this paper the static security assessment (SSA) of the Ethiopian Electric Power (EEP) 400kV system through integration of IPFC under N-1 contingency condition is investigated. The Bus and line loading-based composite severity indices (CSI) were utilized to determine the state of the system and to get an optimal location for interline power flow controller (IPFC) placement. In this research, the optimal sizing of IPFC was done by using Grey Wolf Optimization (GWO) algorithm for the reason that the proposed approach is simple to formulate and requires less programming effort with better computational efficacy than other complex programming and optimization approaches. From the analysis it was found that the Gelan to Sebeta and Gelan to Holeta branches are found to be with higher voltage instability than the others and identified as the primary bus for IPFC placement. Integrating the 50MVA-rated IPFCs within the system reduced the severity margin of bus voltage violations and line overloading. The possibility of bus voltage magnitude violation and the line-overloading situation is effectively reduced when simulating the system with IPFC. From the findings, the integration of IPFC within the system significantly improved and maintained the static security issues of the proposed power system under N-1 contingency conditions.

6. Future work

This study evaluated the possibility of reducing power system safety problems using IPFC with MATLAB software. However, its effectiveness has not been verified in practice by the researchers because the implementation and practical mitigation strategy requires a large budget and time. Therefore, the practical validity of such scheme will be carried out in future studies. Further, economic analysis of installing IPFC in the system, realistic simulation of EEP HV 400 kV and other systems such as 230 kV, and 132 kV, contingency simulation including N-2 scenario, generation plant outage scenarios and conducting a dynamic security assessment could be considered as future work including verification of safety issues by other power systems simulation software.

Data Availability

The generation plant, line data, and load data used to support the findings of this study are included within the article.

Conflicts of Interest

The authors declare no conflicts of interest regarding the publication of this paper.

References

[1] W. Li, *Risk Assessment of Power Systems Models, Methods, and Applications*, IEEE press, Vancouver, Canada, 2015.

[2] E. Buraimoh, K. Ariyo, and I. Davidson, "Power system static security enhancement through interline power flow controller," in *Proceedings of the IEEE PES/IAS Power Africa*, pp. 330–335, Cape Town, South Africa, June 2018.

[3] T. Kiran and D. M. Vinod, "Power system security assessment and enhancement: a bibliographical survey," *Journal of the Institution of Engineers*, vol. 101, pp. 1–14, 2020.

[4] N. G. Hingorani and L. Gyugyi, *Understanding FACTS: Concepts and Technology of Flexible AC Transmission Systems*, IEEE Press, Piscataway, NJ, USA, 1999.

[5] Nexant, *Grid Management Support Program for System Operation and gap Analysis (SOGA)*, United States Agency for International Development, Washington, D.C., USA, 2019.

[6] G. Mostafa, J. Mohammad, S. Mostafa, A. Mahdi, and R. Mohammadreza, "Static security assessment of power systems: a review," *International Trans Electr Energ Syst*, vol. 30, 2020.

[7] K. Nagesh, B. Sravana, V. Rao, and D. Deepak, "Enhancement of voltage stability using FACTS devices in an electrical transmission system with optimal rescheduling of generators by a brainstorm optimization algorithm," *Brainstorm Optimization Algorithms*, Springer, Berlin, Germany, 2019.

[8] C. Pallavi, S. Sanjay, and A. Siddiqui, "Improvement of power system security under single line critical contingency condition by optimal placement of multiple TCSCs," *Advances in Power Systems and Energy Management*, pp. 701–708, Springer, Berlin, Germany, 2018.

[9] K. V. K. Kavuturu, P. V. R. L. Narasimham, and P. Narasimham, "Transmission security enhancement under (N−1) contingency conditions with optimal unified power flow controller and renewable energy sources generation," *Journal of Electrical Engineering & Technology*, vol. 15, no. 4, pp. 1617–1630, 2020.

[10] K. Tong, J. Yao, T. Duong, S. Yang, and X. Zhu, "A hybrid approach for power system security enhancement via the optimal installation of flexible ac transmission system (FACTS) devices," *Energies*, vol. 10, no. 1305, pp. 1–32, 2017.

[11] F. Frezer, "Transmission line loss minimization and contingency analysis in Ethiopian power system: case study of the

southern region," MSc thesis, Arba Minch University, Arba Minch, Ethiopia, 2021.

[12] M. Natnael, "Assessing transmission line loss in Ethiopian electric power system under contingency conditions," MSc thesis, Addis Abeba University, Addis Ababa, Ethiopia, 2018.

[13] B. Genanew, "Contingency analysis of Ethiopian power system on 230 kV and 400 kV transmission lines," MSc thesis, Bahir Dar University, Bahir Dar, Ethiopia, 2019.

[14] S. Gezahegn, "Studies on Ethiopian high voltage grid security enhancement using UPFC," MSc thesis, Addis Abeba University, Addis Ababa, Ethiopia, 2021.

[15] Y. Li, Y. Li, and Y. Sun, "Online static security assessment of power systems based on lasso algorithm," *Applied Sciences*, vol. 8, no. 9, pp. 1442–1465, 2018, https://www.mdpi.com/2076-3417/8/9/1442?type=check_update&version=1#metrics.

[16] B. Desalegn, O. Ayodeji, and G. Yalew, "Load flow and contingency analysis for transmission line outage," *Archives of Electrical Engineering*, vol. 69, no. 3, pp. 581–594, 2020.

[17] M. Krishna and N. Vijaya, "Post-contingency management of power system in presence of interline power flow controller using line-based indices," *IJIRSET*, vol. 5, no. 11, Article ID 19902, 2016.

[18] Y. Li and Y. Li, "Security-constrained multi-objective optimal power flow for a hybrid AC/VSC-MTDC system with lasso-based contingency filtering," *IEEE Access*, vol. 8, pp. 6801–6811, 2020.

[19] M. Lekshmi and M. Nagaraj, "Online static security assessment module using radial basis neural network trained with particle swarm optimization," in *Proceedings of the ICIEES: International Conference on Intelligent and Efficient Electrical Systems*, Singapore, 2018.

[20] T. Kumar, J. Pal, and K. Chandan, "Multi-dimensional ANN application for active power flow state classification on a utility system," in *Proceedings of the IEEE Calcutta Conference*, Kolkata, India, February 2020.

[21] Sudha and M. S. Sureban, "Contingency analysis of power system using ANN," *International Journal of Scientific Engineering and Research*, vol. 10, no. 5, pp. 90–94, 2019.

[22] S. Mirjalili, S. M. Mirjalili, and A. Lewis, "Grey wolf optimizer," *Advances in Engineering Software*, vol. 69, pp. 46–61, 2014.

[23] E. Gupta and A. Saxena, "Grey wolf optimizer based regulator design for automatic generation control of interconnected power system," *Cogent Engineering*, vol. 3, no. 1, Article ID 1151612, 2016.

[24] V. K. Kamboj, S. K. Bath, and J. S. Dhillon, "Solution of non-convex economic load dispatch problem using grey wolf optimizer," *Neural Computing & Applications*, vol. 27, no. 5, pp. 1301–1316, 2016.

[25] M. Akanksha and N. K. Venkata, "Line utilization factor-based optimal allocation of IPFC and sizing using firefly algorithm for congestion management," *IET Generation, Transmission & Distribution*, vol. 10, pp. 1–8, 2015.

[26] A. Yazdanpanah-Goharrizi and R. Asghari, "A novel line stability index (NLSI) for voltage stability assessment of power systems," in *Proceedings of the 7th WSEAS International Conference on Power Systems*, Venice, Italy, December 2017.

[27] M. Alivelu, *Modeling and control of interline power flow controller for power system stability enhancement*, Ph.D. thesis, University technology Petronas, Perak, Malaysia, 2011.

[28] A. Amarendra, S. Ravi, and S. Rao, "Security enhancement in power system using FACTS devices and atom search optimization algorithm," *EAI Endorsed Transactions on Energy Web*, pp. 1–15, vol. 8, no. 36,, 2021.